

# Deformation effects in toroidal and compression dipole excitations of $^{170}\text{Yb}$ : Skyrme-RPA analysis

J. Kvasil<sup>1</sup>, V.O. Nesterenko<sup>2</sup>, W. Kleinig<sup>2,3</sup>, and P.-G. Reinhard<sup>4</sup>

<sup>1</sup> *Institute of Particle and Nuclear Physics, Charles University, CZ-18000, Prague, Czech Republic*

<sup>2</sup> *Laboratory of Theoretical Physics, Joint Institute for Nuclear Research, Dubna, Moscow region, 141980, Russia\**

<sup>3</sup> *Technische Universität Dresden, Institut für Analysis, D-01062, Dresden, Germany and*

<sup>4</sup> *Institut für Theoretische Physik II, Universität Erlangen, D-91058, Erlangen, Germany*

The effect of nuclear deformation on the isoscalar toroidal and compression dipole modes in prolate  $^{170}\text{Yb}$  is studied in the framework of the random-phase-approximation method with a representative set of Skyrme forces (SV-bas, SLy6, SkM\* and SkI3). It is shown that the deformation crucially redistributes the strength of both modes. The compression mode has the same sequence of  $\mu=0$  and 1 branches as the isovector giant dipole resonance where for prolate nuclei the  $\mu=0$  mode is lower in energy ( $\mu$  being the projection of the axial momentum of the mode). Instead, the toroidal mode exhibits an anomalous (opposite) sequence where the  $\mu=1$  branch precedes the  $\mu=0$  one.

## I. INTRODUCTION

The toroidal and compression modes (TM and CM in what follows) in the isoscalar dipole  $E1(T=0)$  channel represent two unconventional kinds dipole motion, attracting increasing interest last years [1]. Both modes are second-order corrections to the dominant giant dipole resonance (GDR) flow [2]. After extraction of the spurious center-of-mass motion, these modes become dominant in  $E1(T=0)$  channel. TM and CM were observed in  $(\alpha, \alpha')$  scattering experiments [3, 4] where they were treated as the low-energy (TM) and high-energy (CM) branches of the isoscalar dipole giant resonance (ISGDR) [1]. The modes are strongly mixed [1, 2].

The TM is viewed as a toroid-like *vortical* flow [5, 6]. Its restoring force is caused by distortions of the Fermi sphere in the momentum space. So the TM can be treated as a specific transversal oscillation of an elastic globe [7, 8]. As was recently shown [9], the TM lies at the low-energy region of what is called the pygmy dipole resonance (PDR) and determines the basic collective flow in the region. This is important since this low lying strength carries a great deal of information on basic nuclear parameters as incompressibility, symmetry energy, and effective masses [10] which, in turn, is related to questions of the neutron skin and neutron equation-of-state. The CM exhibits an *irrotational* compression dipole flow [11, 12]. Actually, the TM and CM are transversal (vortical) and longitudinal (irrotational) counterparts.

The TM and CM were thoroughly investigated in various models, see extensive references in [1, 2, 13, 14]. Most studies so far were limited to spherical nuclei. At the same time, effects of nuclear deformation in TM and CM can be very strong. As shown in our recent study for the chain of Sm isotopes [14], the deformation appreciably reshuffles the TM/CM strengths. In particular, there was a spectacular deformation splitting (exceeding

5 MeV) of CM and considerable downshift of the TM strength (which can affect the PDR properties).

In this paper, we continue investigation of the deformation effects in TM and CM, now for a typical rare-earth axial nucleus  $^{170}\text{Yb}$  which exhibits a sizable prolate deformation. Like in the previous study [14], we employ the separable random-phase-approximation (SRPA) approach using the Skyrme energy-density functional [15, 16]. SRPA was already successfully used in various studies in spherical and deformed nuclei (electric [2, 14, 17–19] and magnetic [20–22] giant resonances,  $E1$  strength near the particle thresholds [23, 24]). Here we employ it with the Skyrme forces covering various values of isoscalar effective mass  $m_0^*/m$ . These are SV-bas [25], SkM\*[26], SLy6 [27], SkI3 [28] with  $m_0^*/m=0.90, 0.79, 0.69, 0.58$ , respectively. While in our previous study [14] the CM deformation effects were mainly analyzed, here we consider deformation features of both TM and CM. It will be shown that, unlike the isovector giant dipole resonance (GDR) and CM, the TM demonstrates an anomalous deformation splitting. Namely, in TM the dipole branch  $\mu=1$  lies lower than the  $\mu=0$  one, in contrast to the opposite sequence 0/1 typical for prolate quadrupole shapes.

The paper is organized as follows. In Sec. 2 the calculation scheme is outlined. In Sec. 3 the main results are discussed. In Sec. 4, the conclusions are given.

## II. CALCULATION SCHEME

The study is performed within the SRPA approach with the Skyrme functional [15, 16]. The method is fully self-consistent as i) both the mean field and residual interaction are obtained from the same Skyrme functional [29–31], ii) the residual interaction includes all the functional contributions as well as the Coulomb (direct and exchange) terms. The self-consistent factorization of the residual interaction in SRPA dramatically reduces the computational effort for deformed nuclei while keeping high accuracy of the method. As shown in the systematic

---

\*Electronic address: nester@theor.jinr.ru

SRPA study of GDR in rare-earth and actinide regions [18], the method provides an excellent description of the experimental data in a wide manifold of deformed nuclei.

In order to test the sensitivity of the results, four different Skyrme forces (SV-bas [25], SkM\*[26], SLy6 [27], and SkI3 [28]) with various isoscalar effective masses are used. The 2D representation in cylindrical coordinates with a mesh size of 0.7 fm and a calculation box of 21 fm is exploited. The pairing (with delta forces) is treated at the BCS level [32]. The equilibrium axial quadrupole deformation is determined by minimization of the total energy. In  $^{170}\text{Yb}$ , we obtain for all four Skyrme forces the deformation parameter  $\beta_2=0.34-0.35$  and corresponding quadrupole moment  $Q_2 \approx 8.5$  b. These values are in acceptable agreement with the experimental data  $\beta_2^{\text{exp}}=0.32$  and  $Q_2^{\text{exp}}=7.6$  b [33].

The TM and CM strength functions read

$$S_\gamma(E1\mu, E) = \sum_\nu |\langle \nu | \hat{M}_\gamma(E1\mu) | 0 \rangle|^2 \xi_\Delta(E - E_\nu) \quad (1)$$

where  $\xi_\Delta(E - E_\nu) = \Delta/[2\pi((E - E_\nu)^2 + (\Delta/2)^2)]$  is the Lorentz weight with the averaging parameter  $\Delta = 1$  MeV. Further,  $|0\rangle$  is the ground state wave function,  $E_\nu$  and  $|\nu\rangle$  are the energy and wave function of the  $\nu$ -th RPA state.  $\hat{M}_\gamma(E1\mu)$  is the transition dipole operator where  $\gamma$  labels the cases TM, CM, or GDR. The TM and CM operators read [2]:

$$\hat{M}_{\text{tor}}(E1\mu) = -\frac{2}{2c\sqrt{3}} \int d^3r \hat{j}_{\text{nuc}}(\vec{r}) \cdot \left[ \frac{\sqrt{2}}{5} r^2 \vec{Y}_{12\mu} + (r^2 - \delta_{T,0} \langle r^2 \rangle_0) \vec{Y}_{10\mu} \right], \quad (2)$$

$$\hat{M}_{\text{com}}(E1\mu) = \frac{1}{10} \int d^3r \hat{\rho}(\vec{r}) \left[ r^3 - \delta_{T,0} \frac{5r}{3} \langle r^2 \rangle_0 \right] Y_{1\mu}, \quad (3)$$

where  $\hat{\rho}(\vec{r})$  and  $\hat{j}_{\text{nuc}}(\vec{r})$  are operators of nuclear density and convection current, respectively. Symbols  $Y_{\lambda\mu}$  and  $\vec{Y}_{\lambda\mu}$  stand for spherical harmonics and vector spherical harmonics. The value  $\langle r^2 \rangle_0 = \int d^3r \rho_0(\vec{r}) r^2$  is the ground state root-mean-square radius. The last terms in (2) and (3) represent the center-of-mass corrections (c.m.c.) active in T=0 channel [2]. The neutron and proton effective charges in this channel are  $e_n^{\text{eff}} = e_p^{\text{eff}} = 1$ .

The photo-absorption cross-section is determined through the strength function (1) as [34]:

$$\sigma_{\text{phot}}(E1\mu) = \frac{16\pi^3 \alpha_e}{9e^2} E \cdot S_{\text{GDR}}(E1\mu, E) \quad (4)$$

where  $\alpha_e = 1/137$  is the fine-structure constant and

$$\hat{M}_{\text{GDR}}(E1\mu) = \frac{N}{A} \sum_{p=1}^Z r_p Y_{1\mu}(\hat{r}_p) - \frac{Z}{A} \sum_{n=1}^N r_n Y_{1\mu}(\hat{r}_n) \quad (5)$$

is the standard dipole isovector (T=1) transition operator.

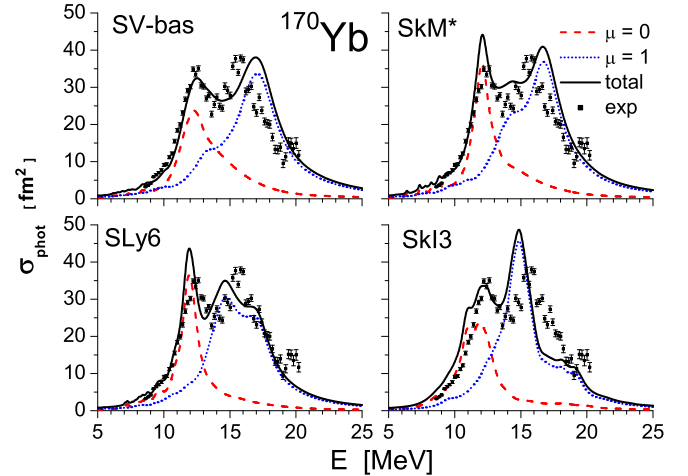


FIG. 1: (color online) The SRPA total (black solid) and partial  $\mu=0$  (red dash) and  $\mu=1$  (blue dotted) photo-absorption cross sections in  $^{170}\text{Yb}$ , computed for various Skyrme forces as indicated. The experimental data [37, 38] are depicted by black full squares.

The total strengths (1) and (4) are computed as the sums of  $\mu=0$  and twice the  $\mu=1$  contributions. The input SRPA operators are chosen following the prescription [2].

The configuration space for the SRPA calculations covers all the two-quasiparticle dipole states with the energy up to  $E_{\text{cut}} \approx 175$  MeV. The basis is sufficiently large to exhaust nearly 100% of the energy-weighted sum rules (EWSR): i) Thomas-Reiche-Kuhn EWSR (T=1) for GDR [34] and ii) Harakeh's EWSR (T=0) for CM [35]. We need also this large basis to lower the energy of the spurious E1 (T=0) peak (c.m. mode) towards its zero value. Here the spurious peak comes down to 1.5–3.0 MeV (depending on the Skyrme force) for CM and close to zero for TM. This is safely below the regions of the studied TM and CM strengths. Note that TM, driven mainly by vortical flow, is generally less polluted by the spurious motion than the irrotational CM. An extensive discussion of the sum rules and c.m. correction in SRPA calculations can be found in Ref. [14]. Other details of the calculation scheme are given elsewhere [2, 16, 18].

### III. RESULTS AND DISCUSSION

In Figure 1, the photo-absorption cross section calculated with different Skyrme forces is compared to the experimental data [37, 38]. Decomposition of the dipole strengths into  $\mu=0$  and  $\mu=1$  branches is also given to demonstrate the deformation splitting. The figure shows a good agreement with the experiment for all the Skyrme forces. The energy position, width and splitting of the GDR are well reproduced. At the same time, the dependence of the description on the Skyrme force is also

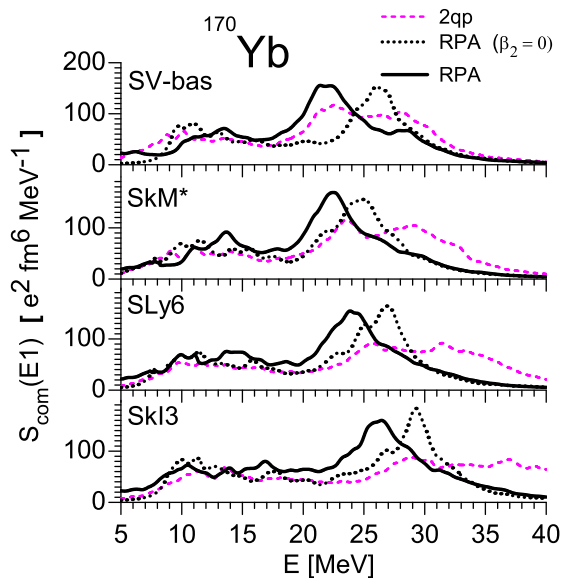


FIG. 2: (color online) Compression E1(T=0) strength functions in  $^{170}\text{Yb}$ , calculated with different Skyrme parametrizations. The 2qp (red dash), RPA (black solid) and constrained (by the spherical nuclear shape with  $\beta_2=0$ ) RPA (blue dotted) strengths are depicted.

visible. A minor narrowing the GDR and downshift of  $\mu=1$  branch from SV-bas to SkI3 (i.e. with decreasing the effective mass  $m_0^*/m$ ) are seen. They can be understood from the fact that the level density of the single-particle spectra decreases with decreasing  $m_0^*/m$  [36]. SV-bas somewhat overestimates the GDR width and  $\mu=1$  energy while SkI3 underestimates these values. The best result is obtained for SLy6 with  $m_0^*/m=0.69$ , which is in accordance to our previous findings for the GDR within SRPA [18]. The deformation splitting shows the standard ordering for the GDR in prolate nuclei where the peak for  $\mu=0$  lies energetically lower than the  $\mu=1$  peak.

In Figure 2, the CM E1(T=0) strength is presented. The RPA residual interaction significantly downshifts the strength as compared with the unperturbed two-quasiparticle (2qp) spectra, which indicates a considerable collectivity of the excitations. Like in Fig. 1 for GDR, there is a visible regular dependence of the energy of the main CM peak on the Skyrme force, which is explained by the compression of the single-particle spectrum with increasing  $m_0^*/m$ . Fig. 2 shows a strong impact of deformation. As compared with the spherical case (RPA on a ground state with constraint on  $\beta_2=0$ ), the deformation downshifts the low-energy strength to the region 5-8 MeV. Besides, the main CM peak is shifted from 26-30 MeV to 22-26 MeV. Similar effects were earlier found for CM in Sm isotopes [14].

More information on the impact of deformation on the

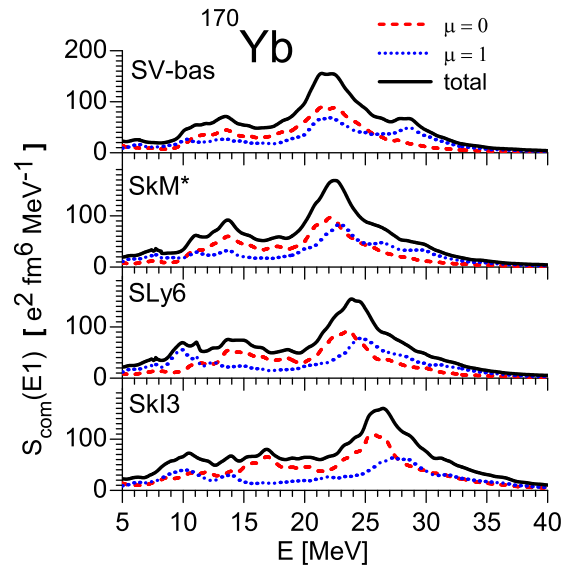


FIG. 3: (color online) The total (solid black),  $\mu=0$  (red dash), and  $\mu=1$  (blue dotted) RPA E1(T=0) compression strength functions in  $^{170}\text{Yb}$ , calculated with different Skyrme parametrizations.

CM can be obtained from Fig. 3, where the total RPA strength is given together with its  $\mu=0$  and 1 branches. It is seen that the deformation drastically redistributes the strength, making the ratio between  $\mu=0$  and 1 strengths dependent on the energy (while in the spherical case this ratio is constant). In particular, we get the dominance of  $\mu=0$  strength at the central energy region 10-25 MeV and of  $\mu=1$  strength at the peripheral regions at lower and higher energies. If one considers the major and minor CM peaks at 22-26 and 26-32 MeV as  $\mu=0$  and  $\mu=1$  branches, then one may state a considerable (though vague) deformation splitting. The splitting changes from  $\sim 7$  MeV in SV-bas to  $\sim 2$  MeV in SkI3. Like in the GDR, the deformation splitting exhibits the 0/1 order where the  $\mu=0$  bump precedes the  $\mu=1$  one.

Figures 4 and 5 illustrate the strength functions for TM. As compared to high-energy CM, the TM strength is mainly concentrated at lower energy 5-20 MeV. There is also a minor TM high-energy bump at 20-30 MeV, perhaps because of the CM and TM coupling. In Fig. 4, we see the similar effects as in Fig. 2 for CM: i) downshift of the RPA strength as compared to 2qp case, ii) strong redistribution of the RPA strength due to deformation (including a shift of the strength to the low-energy region below 7-8 MeV and also a downshift of the minor high-energy bump), and iii) visible dependence of the TM centroid on  $m_0^*/m$ .

In Figure 5, we see a remarkable strong effect of deformation on the low-energy TM: the deformation splitting

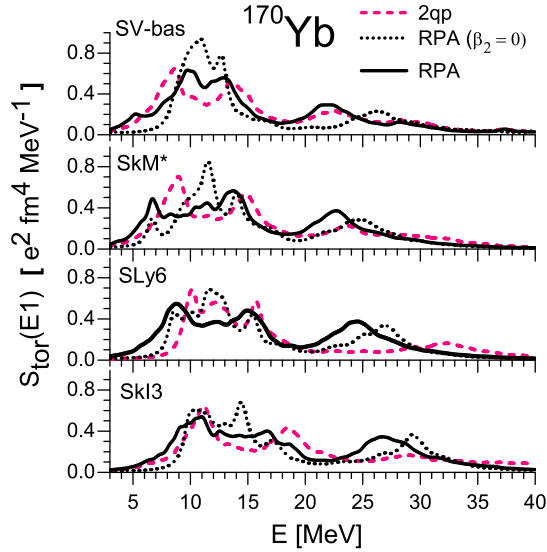


FIG. 4: (color online) The same as in Fig. 2 but for the toroidal  $E1(T=0)$  strengths.

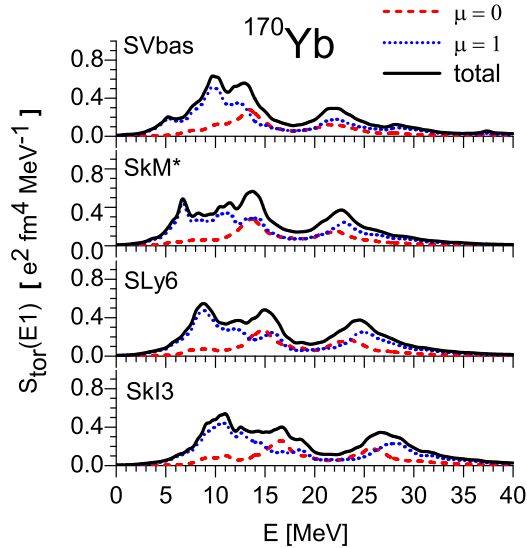


FIG. 5: (color online) The same as in Fig. 3 but for the toroidal  $E1(T=0)$  RPA strengths.

results in an overwhelming dominance of  $\mu=1$  branch in the TM strength below 12-15 MeV. This is in contrast to the GDR where, following Fig. 1, the  $\mu=0$  branch dominates at  $E < 13$  MeV. Moreover, TM has the opposite order of the branches as compared to the GDR and CM ( $\mu = 1$  is lower than  $\mu = 0$ ). The difference takes

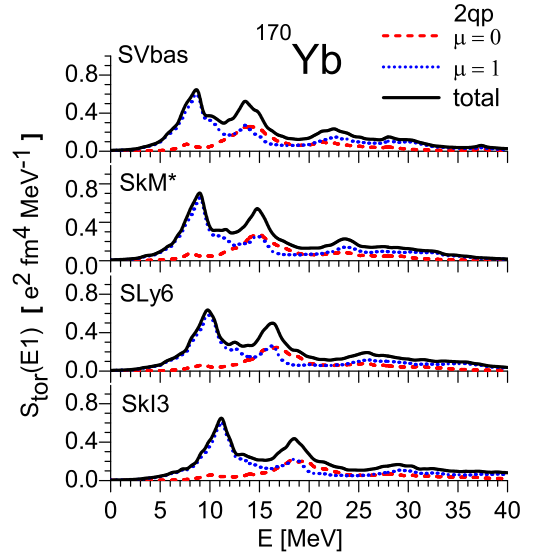


FIG. 6: (color online) The same as in Fig. 3 but for the toroidal  $E1(T=0)$  2qp strengths.

place in spite of the fact that both, TM and GDR, originate from the same 2qp dipole transitions with  $\Delta N=1$ , where  $N$  is the principle shell quantum number. As seen from Fig. 6, the effect appears already for the unperturbed 2qp strength and therefore has its origin in the mean field and not in the recoupling by RPA. Perhaps it is caused by a different character of the flows in TM and GR (vortical and irrotational, respectively) and thus different 2qp excitations generating TM and GDR. This effect calls for a careful microscopical analysis which is the next step on our road map.

#### IV. CONCLUSIONS

The effects of nuclear axial quadrupole deformation on the isoscalar dipole compression and toroidal modes (CM and TM) were investigated in prolate  $^{170}\text{Yb}$  within the random-phase approximation using the Skyrme energy-density functional. The Skyrme parametrization SV-bas [25], SkM\*[26], SLy6 [27], and SkI3 [28] were used which have different isoscalar effective mass  $m_0^*/m$  varying from 0.9 for SV-bas to 0.58 for SkI3. All four forces provide similar general pattern, but visible dependence on  $m_0^*/m$  in the details of the spectral distributions.

The strong impact of deformation found here is in accordance with our previous study for Sm isotopes [14]. The deformation significantly redistributes the strengths, in particular the ratios between  $\mu=0$  and 1 branches. The  $\mu=0$  strength becomes dominant in a wide central region while the  $\mu=1$  strength takes the lead at lower and higher energy.



The most interesting deformation effect takes place for the low-energy TM where an anomalous sequence (as compared to the giant dipole resonance and CM) of the  $\mu=0$  and 1 branches is found. Namely, in contrast to the common order in prolate nuclei, for the TM the  $\mu=1$  branch comes energetically lower than the  $\mu=0$  one. This leads to a strong dominance of  $\mu=1$  over  $\mu=0$  at the energy  $E < 12$ -15 MeV (often associated with the region of the pygmy dipole resonance). This feature was also found in other prolate nuclei (not shown in the paper). Perhaps it is caused by a different character of the modes, vortical flow for the TM and irrotational flow for the GDR, and thus different isoscalar two-quasiparticle excitations generating these flows.

## Acknowledgments

The work was partly supported by the DFG RE 322/14-1, a GSI F+E, Heisenberg-Landau (Germany - BLTP JINR), and Votruba - Blokhintsev (Czech Republic - BLTP JINR) grants. W.K. and P.-G.R. are grateful for the BMBF support under contracts 05P12ODDUE. The support of the research plan MSM 0021620859 (Ministry of Education of the Czech Republic) and the Czech Science Foundation project P203-13-07117S are also appreciated.

- 
- [1] N. Paar, D. Vretenar, E. Khan, and G. Colo, Rep. Prog. Phys. **70**, 691 (2007).
- [2] J. Kvasil, V.O. Nesterenko, W. Kleinig, P.-G. Reinhard, and P.Vesely, Phys. Rev. C**84**, 034303 (2011).
- [3] D.H. Youngblood, Y.W. Lui, H.L. Clark, B. John, Y. Tokimoto, X. Chen, Phys. Rev. C **69**, 034315 (2004).
- [4] M. Uchida *et al.*, Phys. Rev. C **69**, 051301(R) (2004).
- [5] V.M. Dubovik and A.A. Cheshkov, Sov. J. Part. Nucl. **5**, 318 (1975)
- [6] S.F. Semenko, Sov. J. Nucl. Phys. **34**, 356 (1981).
- [7] S.I. Bastrukov, S. Misicu, V.I. Sushkov, Nucl. Phys. A **562**, 191(1993).
- [8] S. Misicu, Phys. Rev. C **73**, 024301 (2006).
- [9] A. Repko, P.-G. Reinhard, V.O. Nesterenko, and J. Kvasil, Phys. Rev. C**87**, 024305 (2013).
- [10] P.-G. Reinhard and W. Nazarewicz, Phys. Rev. C **87**, 014324 (2013).
- [11] M.N. Harakeh *et al.*, Phys. Rev. Lett. **38**, 676 (1977).
- [12] S. Stringari, Phys. Lett. B**108**, 232 (1982).
- [13] J. Kvasil, N. Lo Iudice, Ch. Stoyanov, and P. Alexa, J. Phys. G: Nucl. Part. Phys. **29**, 753 (2003).
- [14] J. Kvasil, V.O. Nesterenko, W. Kleinig, D. Bozik, P.-G. Reinhard, and N. Lo Iudice, Eur. Phys. J. A**49**, 119 (2013).
- [15] V.O. Nesterenko, J. Kvasil, and P.-G. Reinhard, Phys. Rev. C**66**, 044307 (2002).
- [16] V.O. Nesterenko, W. Kleinig, J. Kvasil, P. Vesely, P.-G. Reinhard, and D.S. Dolci, Phys. Rev. C**74**, 064306 (2006).
- [17] V.O. Nesterenko, W. Kleinig, J. Kvasil, P. Vesely, and P.-G. Reinhard, Int. J. Mod. Phys. E**16**, 624 (2007); *ibid* E**17**, 89 (2008).
- [18] W. Kleinig, V.O. Nesterenko, J. Kvasil, P.-G. Reinhard, and P. Vesely, Phys. Rev. C**78**, 044313 (2008).
- [19] J. Kvasil, A. Repko, V.O. Nesterenko, W. Kleinig, and P.-G. Reinhard, Int. J. Mod. Phys. E**21**, 1250041 (2012).
- [20] P. Vesely, J. Kvasil, V.O. Nesterenko, W. Kleinig, P.-G. Reinhard, and V.Yu. Ponomarev, Phys. Rev. C**80**, 031302(R) (2009).
- [21] V.O. Nesterenko, J. Kvasil, P. Vesely, W. Kleinig, P.-G. Reinhard, and V.Yu. Ponomarev, J. Phys. G: Nucl. Part. Phys. **37**, 064034 (2010).
- [22] V.O. Nesterenko, J. Kvasil, P. Vesely, W. Kleinig, and P.-G. Reinhard, Int. J. Mod. Phys. E**19**, 558 (2010).
- [23] J. Kvasil, P. Vesely, V.O. Nesterenko W. Kleinig, P.-G. Reinhard, and S. Frauendorf, Int. J. Mod. Phys. E**18**, 975 (2009).
- [24] J. Kvasil, V. O. Nesterenko, W. Kleinig, D. Božík, and P.-G. Reinhard, Int. J. Mod. Phys. E**20**, 281 (2011).
- [25] P. Kluepfel, P.-G. Reinhard, T.J. Buervenich, and J.A. Maruhn, Phys. Rev. C**79**, 034310 (2009).
- [26] J. Bartel, P. Quentin, M. Brack, C. Guet, and H.-B. Haakansson, Nucl. Phys. A**386**, 79 (1982).
- [27] E. Chabanat, P. Bonche, P. Haensel, J. Meyer, and R. Schaeffer, Nucl. Phys. A**627**, 710 (1997).
- [28] P.-G. Reinhard and F. Flocard, Nucl. Phys. A**584**, 467 (1995).
- [29] T.H.R. Skyrme, Phil. Mag. **1**, 1043 (1956).
- [30] D. Vauterin, D.M. Brink, Phys. Rev. C**5**, 626 (1972).
- [31] M. Bender, P.-H. Heenen, P.-G. Reinhard, Rev. Mod. Phys. **75**, 121 (2003).
- [32] M. Bender, K. Rutz, P.-G. Reinhard, J.A. Maruhn, Eur. Phys. J. A **8**, 59 (2000).
- [33] S. Raman, At. Data Nucl. Data Tables **36**, 1 (1987).
- [34] P. Ring, P. Schuck, Nuclear Many Body Problem, (Springer-Verlag, New York, 1980).
- [35] M.N. Harakeh, A. van der Woude, *Giant Resonances* (Clarendon Press, Oxford, 2001).
- [36] V.O. Nesterenko, V.P. Likhachev, P.-G. Reinhard, V.V. Pashkevich, W. Kleinig, J. Mesa, Phys. Rev. C**70**, 057304 (2004).
- [37] G. M. Gurevich, L. E. Lazareva, V. M. Mazur, S. Yu. Merkulov, G. V. Solodukhov, and V. A. Tyutin, Nucl. Phys. A**351**, 257 (1981).
- [38] A. M. Goryachev and G. N. Zalesnyy, Vopr. Teor. Yad. Fiz. **5**, 42 (1976).